sustainability

MDPI

Article

Large-Deformation Failure Mechanism and Stability Control of a Swelling Soft Rock Roadway in a Sea Area: A Case Study in Eastern China

Ling Dong [1], Dong Wang [1,2,*], Xiaoming Sun [2], Yujing Jiang [1], Hengjie Luan [1], Huichen Xu [3], Baocheng Li [1] and Feng Cai [4]

1 State Key Laboratory of Mining Disaster Prevention and Control Co-Founded by Shandong Province and the Ministry of Science and Technology, Shandong University of Science and Technology, Qingdao 266590, China
2 State Key Laboratory for Geomechanics and Deep Underground Engineering, China University of Mining and Technology, Beijing 100083, China
3 College of Mechanical and Architectural Engineering, Taishan University, Taian 271000, China
4 China National Coal Group Corporation, Beijing 100120, China
* Correspondence: wdwinter@163.com

Abstract: Coal mining in sea areas has higher requirements for geological support systems, technical equipment levels, and safety production capacities because of the complex engineering geological conditions of underwater coal mines. In this paper, the deformation failure mechanism and stability control of a typical swelling soft rock roadway in the Beizao coal mine in a sea area are studied. A series of mechanical experiments and theoretical analyses were conducted to research the mechanical properties and reasons for the deformation failure of the swelling soft rock roadway. The type of the large-deformation failure mechanism of the soft rock roadway was identified as type III_{ABC}, which could be converted to a simple one, such as type II_B. The proposed stability control measure, containing constant-resistance large-deformation bolts, steel mesh, floor hollow grouting cables, and steel fiber concrete, was applied to the site. A good supporting effect was achieved, which could provide a beneficial reference for swelling soft rock roadways in sea areas.

Keywords: swelling soft rock roadway; large-deformation failure mechanism; constant-resistance large-deformation bolt; coal mine in sea area

check for updates

Citation: Dong, L.; Wang, D.; Sun, X.; Jiang, Y.; Luan, H.; Xu, H.; Li, B.; Cai, F. Large-Deformation Failure Mechanism and Stability Control of a Swelling Soft Rock Roadway in a Sea Area: A Case Study in Eastern China. *Sustainability* **2023**, *15*, 5323. https://doi.org/10.3390/su15065323

Academic Editors: Fan Feng, Eryu Wang and Ruifeng Huang

Received: 10 February 2023
Revised: 9 March 2023
Accepted: 14 March 2023
Published: 17 March 2023

1. Introduction

According to the Statistical Review of World Energy in 2022, published by BP p.l.c., coal was the second largest energy source in 2021, accounting for 26.9% of total primary energy consumption, slightly lower than 27.2% in the previous year [1]. The Statistical Bulletin on National Economic and Social Development 2022, published by the National Bureau of Statistics, reported that coal consumption accounted for 56.2% of the total energy consumption in China [2]. Coal resources will remain the dominant energy source for some time in China [3,4].

The amount of coal located underwater is about 4 billion tons, thus occupying a very large proportion of coal reserves and being an important supplement to land coal resources [5,6]. Safety problems in deep mining and major disaster prevention were written into the 14th Five-Year Plan of China [3]. The safe and efficient mining of deep coal resources is one of the important issues of concern for China's energy strategy security [3–9]. Coal mining in the sea area has higher requirements for geological support systems, technical equipment levels, and safety production capacities because of the complex engineering geological conditions of underwater coal mines [10–13].

Compared with conventional coal mines located at the same depth on land, coal mines in sea areas exhibit more significant nonlinear large-deformation phenomena [14–19]. Swelling soft rock is a typical rock stratum in coal mines in the sea area in eastern China.

Swelling soft rock refers to soft rock whose water content or volume changes because of physical and chemical reactions with water [20–22]. The swelling soft rock engineering problem has become one of the most complex theoretical and engineering problems in rock mechanics and engineering geology because of its complicated properties and serious engineering hazards [21–27]. As a result of the impact of water on both the coal and the surrounding rocks, their strength parameters decrease. This makes the swelling soft rock engineering problem more complicated. The deformation mechanism and stability control adopted in roadways on land cannot fully meet the demand of the mining of swelling soft rock roadways in sea area coal mines.

In this paper, the deformation and failure of the swelling soft rock roadway in the Beizao coal mine under original support conditions are investigated and the large-deformation failure mechanism summarized and analyzed. The proposed stability control method was applied to the site. A good supporting effect was achieved, which can provide a beneficial reference for similar roadway support in sea areas.

2. Geological Condition

2.1. Lithological Analysis of the Surrounding Rock

The Beizao coal mine is located in Yantai City, Shandong Province, eastern China (Figure 1). The coal mine covers an area of 29.63 km^2, including a local area of 10.39 km^2 and a sea area of 19.24 km^2. The swelling soft rock roadway being studied in this work is at the elevation of -300 m in the land area and at the elevation of -11 m in the Bohai Sea. There are two major aquifers in the coal mine: a marl aquifer and a mudstone and marl interbedded aquifer. The marl aquifer is at an elevation of -122 m. The mudstone and marl interbedded aquifer is at an elevation of -161 m. These two aquifers have little effect on the research roadway excavation.

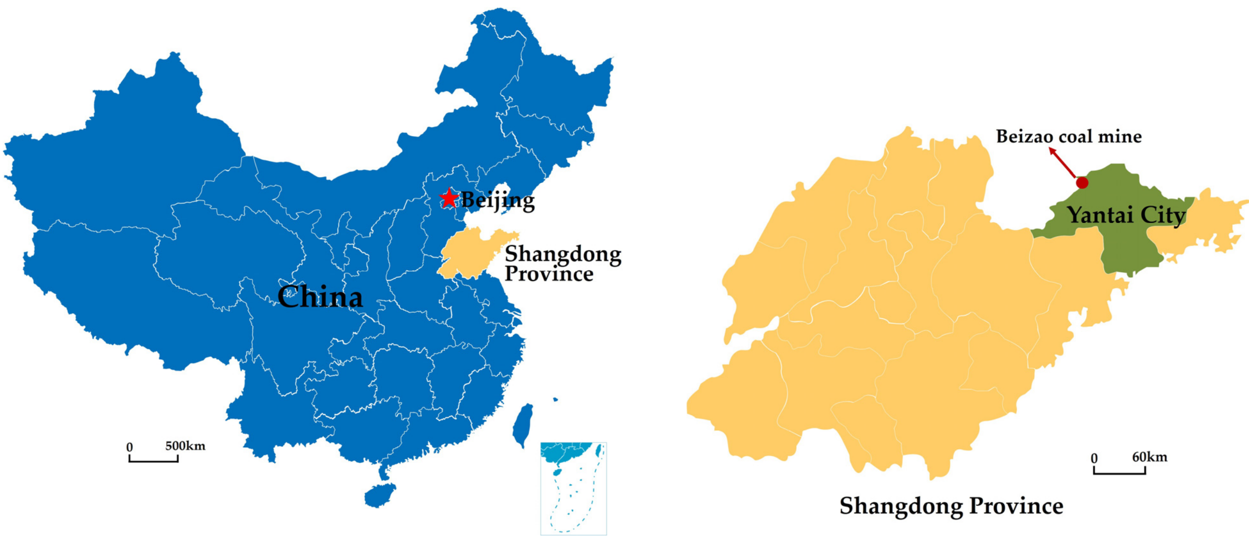

Figure 1. Location of Beizao coal mine.

The lithological profile of the coal seam and the surrounding rock is shown in Table 1. The roof is mainly oily mudstone, and the floor is mainly sand–mudstone. The dip angle of the strata is 6 degrees. The mechanical parameters of the rock samples, as obtained through a series of indoor mechanical experiments, are shown in Table 2. The average compressive strength of the oily mudstone was 6.57 MPa and that of the sand–mudstone was 7.45 MPa, thus indicating an extremely soft, low-strength rock. Mechanical experiments of the surrounding rocks show that the strength of roof and floor rock in the dry state is much higher than that in the natural state by nearly 2.43 times (Figure 2). Thus, water had a large effect on the strength of the surrounding rocks. The water absorption of the oily mudstone is 42.60% and that of the sand–mudstone is 64.21%, thus being in the range of strong water absorption. The swelling rate of the oily mudstone is 15.10% and that of the sand–mudstone is 21.50%, thus being in the high absorption range. Therefore, the soft rock is the typical swelling soft rock, which has low strength, strong water absorption, and high absorption [20–22]. With the special properties of the swelling soft rock, the stability of the rock strata is easily affected by water. The rapid decrease in the strength of the surrounding rock leads to the overall failure of the soft rock roadway, thereby threatening the safety and stability of the entire coal mine.

Table 1. Lithological profile of the coal seam and the surrounding rock.

Lithology	Thickness/m	Geological Description
Oil shale	3.38	Brown grey, oil content is high in the upper part
Oily mudstone	15.87	Compact rock formation, blocky structure, upper horizontal bedding, lower bedding developed, locally containing soft clay interlayer
Coal-2	4.45	Brown black, notably bright coal, followed by dull coal
Sand–mudstone	12.40	Mudstone or fine sandstone with blocky structure, loose mudstone easily swells when exposed to water

Table 2. Mechanical parameters of the surrounding rock.

Location	Lithology	Compressive Strength	Water Absorption	Swelling Rate
Roof	Oily mudstone	6.57 MPa	42.60%	15.10%
Floor	Sand–mudstone	7.45 MPa	64.21%	21.50%

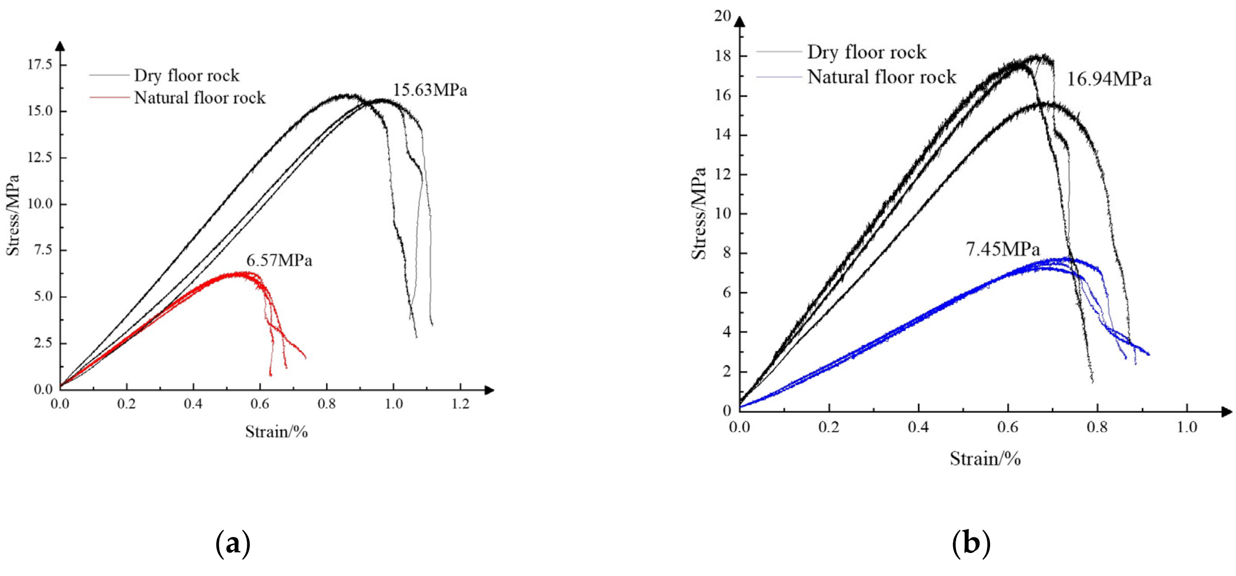

Figure 2. Stress–strain curves of surrounding dry and natural rocks: (**a**) roof rock, oily mudstone; (**b**) floor rock, sand-mudstone.

2.2. Clay Mineral Composition Analysis of the Surrounding Rock

With the different composition and content of clay minerals, soft rock has different structural, physical, and chemical properties, hydrologic properties, and mechanical properties. Therefore, the whole rock mineral composition and content of clay minerals need to be examined through X-ray diffraction experiments. The analysis results of the whole rock minerals are shown in Table 3, and those of the mineral composition and content of clay minerals are shown in Table 4.

Table 3. Results of the whole rock minerals.

Location	Lithology	Species and Content (%) of Mineral					Total Clay Mineral Content (%)
		Quartz	Orthoclase	Albite	Pyrite	Halite	
Roof	Oily mudstone	16.0	/	8.5	0.7	1.4	73.4
Floor	Sand–mudstone	53.7	22.3	9.0	/	/	15.0

Table 4. Results of the clay minerals.

Location	Lithology	Relative Contents of the Clay Minerals (%)						Mixture Layer Ratio (S, %)	
		S	I/S	I	K	C	C/S	I/S	C/S
Roof	Oily mudstone	79	/	4	17	/	/	/	/
Floor	Sand–mudstone	/	19	3	78	/	/	40	/

The analytical data in Table 3 show that the roof contained a large amount of clay minerals (73.4%). Among the clay minerals, smectite had the largest content of 79.0%. The floor was composed of 15% clay minerals. Among the clay minerals, kaolinite had the largest content of 78.0%, and the illite/smectite mixture layer made up 40% of the total content. The mechanical properties of soft rocks are greatly determined by the presence of clay minerals. Typical soft rocks have a large proportion of illite and smectite and a illite/smectite mixture layer; thus, they have significant water absorption and strong swelling. Swelling soft rocks are characterized by softening, disintegration, and swelling when they come into contact with water [20,22–26]. Their strength will then weaken significantly, and a large swelling force will be generated. This condition is highly detrimental to the stability of the swelling soft rock roadway, especially in sea areas. For this reason, stability control of swelling soft rock coal mines in sea areas requires sufficient attention.

2.3. Microstructural Analysis of the Surrounding Rock

The clay minerals in the rock and the structural planes of the rock are the main reasons soft rocks can have significant plastic deformation. Both factors have influential impacts on the engineering mechanical properties of rock mass [24–27]. The microstructures of deep soft rocks appear to have typical specific structural properties that are distinct from those of similar shallow rocks [28–32].

When the oily mudstone was magnified by 2000 times, surface dissolution pores were approximately 20 and 30 μm (Figure 3a), and a micropore with a diameter of 20 μm was observed (Figure 3b). At 1500 times magnification, the sand–mudstone sample appeared to have orthoclase and a microcrack of about 50 μm (Figure 3c). A large dissolution crack with a length of approximately 100 μm and many intergranular pores could be observed at 500 times magnification (Figure 3d).

Some characteristics of the swelling soft rock could be derived from the electron microscope scanning images: (1) The rock structure was loose, and the pores were developed; (2) large quantities of dissolution holes were found on the surface of the mineral, and the pore types were mostly intergranular pores and micropores between clay minerals; and (3) the microfissures were well developed, and some fissures were connected.

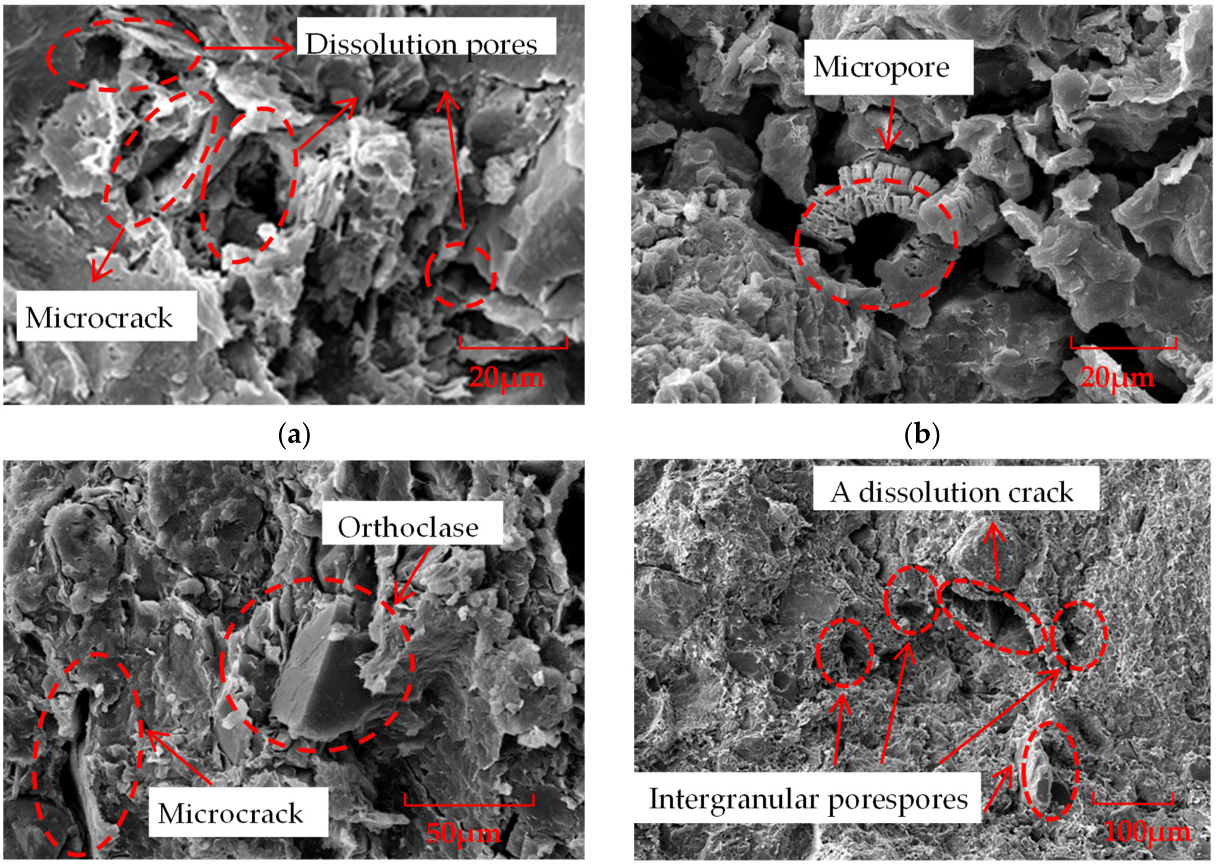

(a) (b) (c) (d)

Figure 3. Electron microscope scanning images of the surrounding rock: (**a**) roof rock, oily mudstone; (**b**) roof rock, oily mudstone; (**c**) floor rock, sand-mudstone; (**d**) floor rock, sand-mudstone.

3. Nonlinear Large-Deformation Mechanism

3.1. Phenomena and Characteristics of Nonlinear Large Deformation

The old support methods adopted the support of U-shaped steel sheds + pouring concrete + steel mesh + shotcrete. U36-shaped steel was used with a spacing of 800 mm. Then, concrete with a thickness of 300 mm was poured into the shed. The regular size of a piece of steel mesh is 2000 × 800 mm. The strength of the shotcrete is C20. Under the old support technology conditions, a great number of typical large-deformation failure phenomena appeared in the roadway. On the basis of a site investigation, the large-deformation failure characteristics can be identified as follows:

(1) Large deformation and shrinkage of all sections of the roadway. Serious roof subsidence occurred for about 800 mm (Figure 4a), and large floor heave deformation occurred for about 900 mm (Figure 4b). The side walls of the roadway also presented obvious shrinkage.
(2) Persistent deformation. The surrounding soft rock is persistently rheological under the complex environment. After more than 10 days of roadway excavation, the surrounding rock still presented persistent large deformation from a macroscopic view.
(3) Failure of the support materials. The concrete layer fell off. The U-shaped steel frames were twisted or destroyed (Figure 4c,d) and were, thus, unable to support the roadway. The support materials utilized were clearly unsuitable for resisting the deformation of the swelling soft rock roadway.

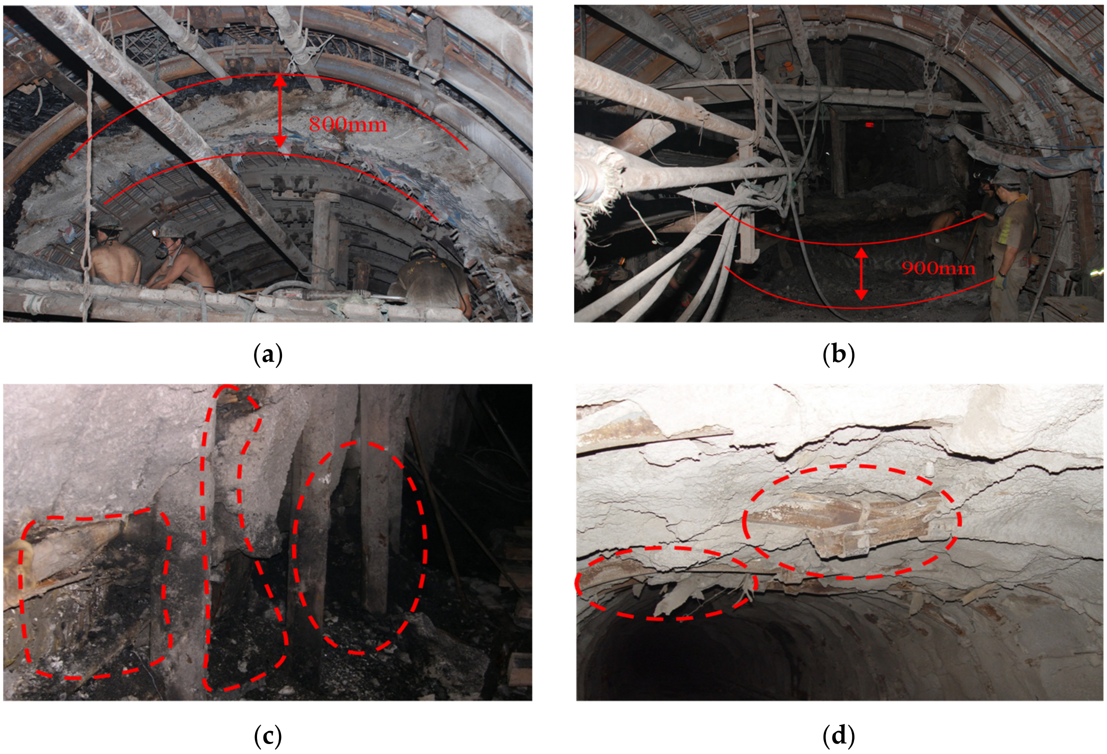

Figure 4. Failure phenomena of the roadway: (**a**) roof subsidence; (**b**) floor heave; (**c**) broken concrete on side walls; (**d**) broken U-shaped steel frame on roof.

3.2. Type of Large-Deformation Failure Mechanism

Many researchers have adopted the typical classification method of the deformation failure mechanism of soft rock roadways proposed by Professor Manchao He [19,20]. On the basis of a field engineering geology study and laboratory mechanics test analyses, the deformation mechanism type of the soft rock roadway can be determined [19–21].

On the basis of the theory of the classification method of the deformation failure mechanism proposed by Professor Manchao He [19,20], the deformation failure mechanism of the swelling soft rock roadway can be analyzed as follows:

(1) Type I is termed a physicochemical expansion type, which is related to the chemical properties of the molecular structure of the soft rock. A significant portion of the mineral composition of the surrounding rocks consists of clay minerals, particularly smectite (79%) and kaolinite (78%). The rock sample also appears to have strong expansibility (Table 2). Therefore, the deformation mechanism in type I can be named type I_{AB}.

(2) Type II is termed a stress expansion type, which is associated with the force source. Tectonic stress in the near horizontal direction and gravitational stress in the vertical direction are the main stresses that act on this roadway. The roadway is in very close proximity to other roadways, generating previous engineering deviatoric stress. Therefore, the deformation mechanism in type II can be named type II_{ABD}.

(3) Type III is termed a structural deformation type, which is related to the combination characteristics of the chamber structure and the rock mass structural plane. The surrounding rock has six faults, a weak intercalated layer, and obvious bedding. The deformation mechanism in type III can be named type III_{ABC}.

The overall deformation mechanism of the swelling soft rock roadway can be identified as the composite mechanism type $I_{AB}II_{ABD}III_{ABC}$.

3.3. Transformation of Nonlinear Large-Deformation Mechanism

Some targeted support measures should be applied to convert the composite mechanism to a simple one [22,23]. The useful mechanical control methods and the specific transformation process are shown in the following steps:

(1) First step: The CRLD bolts make full use of the constant resistance and large deformation by absorbing the energy released by surrounding rocks through deformation. Thus, the composite mechanism of type $I_{AB}II_{ABD}III_{ABC}$ can be converted to type $II_{ABD}III_{ABC}$.
(2) Second step: The combined application of 3000 and 2500 mm long CRLD bolts provides effective control of large deformations, and floor grouting bolts are adopted to enhance the floor support strength. Through these methods, type $II_{ABD}III_{ABC}$ can be transformed to type II_{ABD}.
(3) Third step: The combined use of rock bolts, steel mesh, and anchor beams can improve the support strength. Floor grouting bolts can enhance the strength of the floor. The coupling control methods can play an important role in converting the complex mechanism to a simple type II_B.

The specific transformation process is shown in Figure 5.

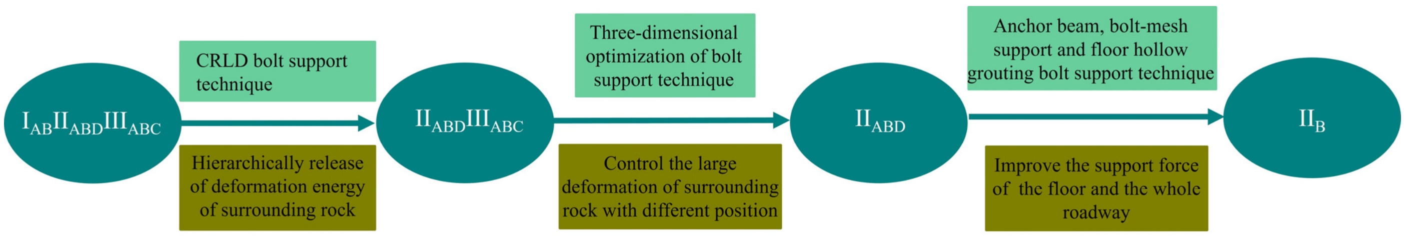

Figure 5. Transformation process of the composite deformation mechanism.

4. Results

4.1. Support Mechanism of CRLD Bolt

CRLD bolts, adopted in the support process in the research, plays a great supporting role. A CRLD bolt is mainly composed of a nut, a pallet, a constant-resistance device, a connection fitting, and a connecting rod [16–18]. Typical features of the CRLD bolt are the high constant resistance and large deformation during the support process. As shown in Figure 6, the average constant resistance is 160 kN, and the average deformation is 761 mm, which is about 48.06% of the length of the bolt. During the support process, it can absorb the energy from the surrounding rock through its deformation. After the deformation, it can also support the surrounding rock effectively. These mechanical properties can give effective support for the roadway. Many mechanical experiments have been conducted in labs and on-site. The properties of high constant resistance and large deformation can meet the support requirements of deep soft rock roadways.

The working mechanism of the CRLD bolt, playing a supporting role in the roadway-surrounding rock, can be divided into the following three stages:

(1) Stage 1: In this stage, the supporting force of the bolt is less than the design resistance value of the CRLD bolt. In the process, the CRLD bolt plays the same supporting role as an ordinary bolt and plays the function of resisting the deformation of the surrounding rock.
(2) Stage 2: In this stage, the CRLD bolt generates deformation, depending on its own constant-resistance device, and the deformation of supporting materials can absorb the energy released by the surrounding rock in the deformation process, making the surrounding rock of the roadway develop into new support in a balanced way.
(3) Stage 3: In this stage, the deformation energy of the surrounding rock gradually decreases after the deformation of the surrounding rock. Under the support of CRLD

bolts, the surrounding rock of the roadway reaches a new equilibrium and stable state again.

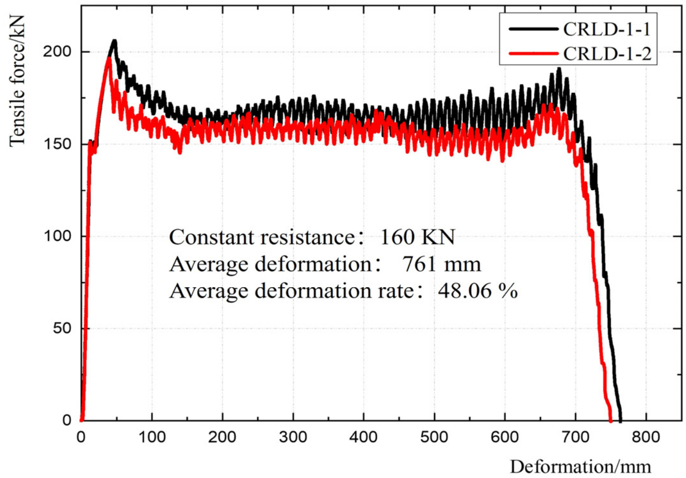

Figure 6. Tensile force and deformation curve of static tensile experiment of CRLD bolts.

4.2. Stability Control and Application

A new multiple stability control method of CRLD bolts + anchor beam + steel mesh + floor grouting bolts + steel fiber concrete is presented based on the transformation process of the mechanism and the corresponding countermeasures. The sectional support design of the new support countermeasures is shown in Figure 7. The support materials and parameters of the new support countermeasure are as follows:

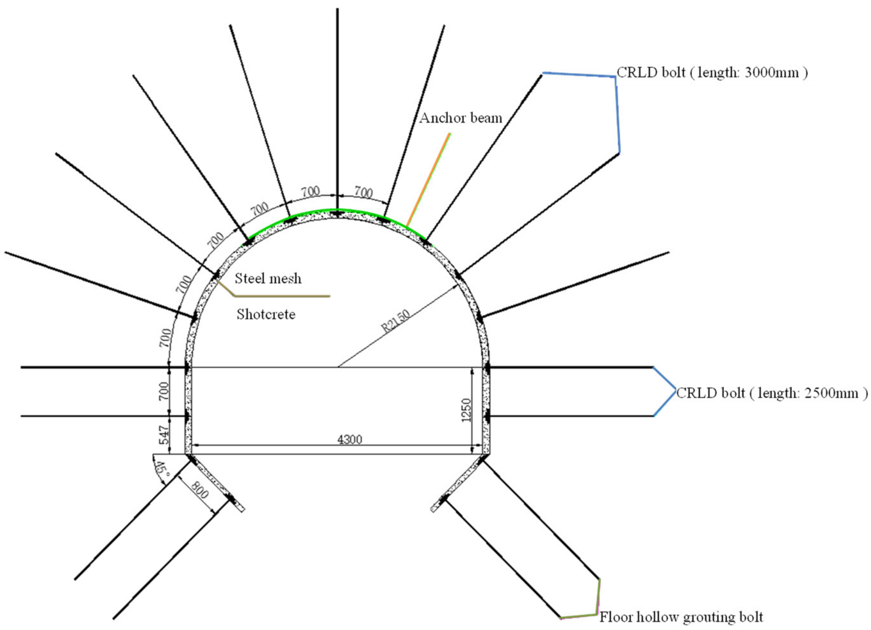

Figure 7. Sectional support design of the new support countermeasure.

A new multiple stability control method of CRLD bolts + anchor beam + steel mesh + floor grouting bolts + steel fiber concrete is presented based on the transformation process of the mechanism and the corresponding countermeasures. The sectional support design of the new support countermeasures is shown in Figure 6. The support materials and parameters of the new support countermeasure are as follows:

(1) Bolt: Two sizes of CRLD bolts were used—one with a length of 3000 mm and the other with a length of 2500 mm. These CRLD bolts were aligned in parallel, with a space of 700 × 700 mm between them.
(2) Anchor beam: U-shaped steel beams were adopted, each with a length of 3000 mm. They were processed into an arc shape to match the section geometry of the roadway. Each anchor beam was fastened with four 3000 mm long CRLD bolts. The bolt holes on the beam were processed into an oval shape.
(3) Floor grouting bolt: Two 3000 mm long hollow floor grouting bolts were placed in each corner of the floor. The bolts were aligned in parallel, and the space between the rows of each bolt was 800 × 700 mm.
(4) Steel mesh: The diameter of the steel mesh is 8.0 mm. Each piece has a conventional size of 800 × 2200 mm, which consists of many small squares with a size of 100 × 100 mm. The overlapped portion of the connection part is 100 mm.
(5) Concrete: Steel fiber concrete with a strength of C20 was used.

The sectional support design of the old support countermeasures is shown in Figure 8. The support materials are U-shaped steel frames, rebar bolts, and shot-concrete.

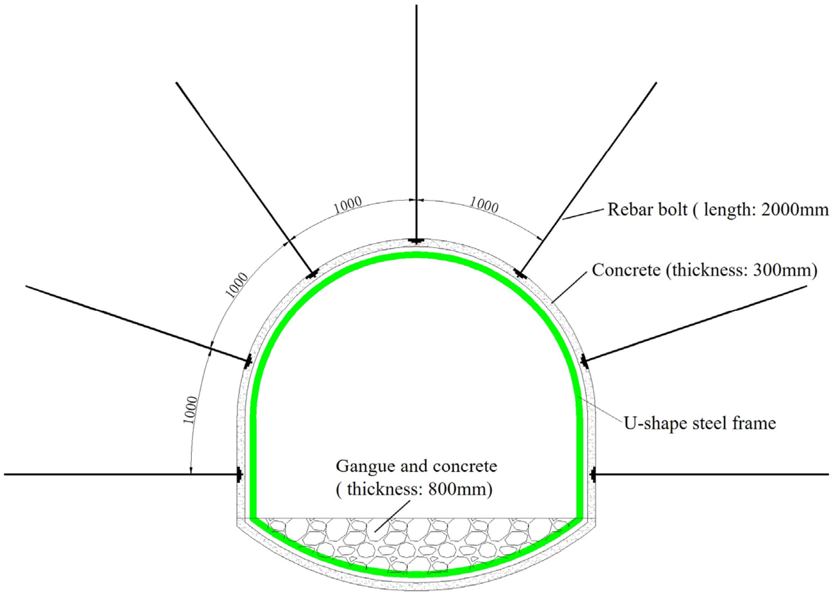

Figure 8. Sectional support design of the old support countermeasure.

4.3. Support Effect of the New Support Countermeasure

The deformation of the surrounding rock of the roadway was monitored by a roadway dynamic measuring instrument to test the effectiveness of the support design. The instrument could automatically monitor and record the deformation data of the roof, floor, and sidewalls. As shown in Figure 9, four monitoring points were set on the new support test section of the roadway, and two monitoring points were set on the old support test section. The deformation of the roadway surface is shown in Figure 10. The deformation process can be classified into two stages: excavating stage I and mining stage II.

(1) In excavating stage I, the deformation situation had three stages: the active stage, transitional stage, and stable stage. After the fast deformation of the I1 and I2 stages, the total deformation of the surrounding rock appeared stable, which was the stable stage of I3.
(2) In mining stage II, the deformation situation of the surrounding rock also had three stages under the impact of the mining of the working face. In the first stage, II1, the deformation rate was slow, and the deformation value was small. In the second stage, II2, the deformation rate became faster. The total deformation value became larger than that in stage II1. The deformation was the greatest. In stable stage II3, the

deformation rate was zero, and the total deformation was a stable value. It is clear that the amount of the deformation of this stage is much greater than that of excavating stage I, and the lasting time of this stage is much less than that of excavating stage I.

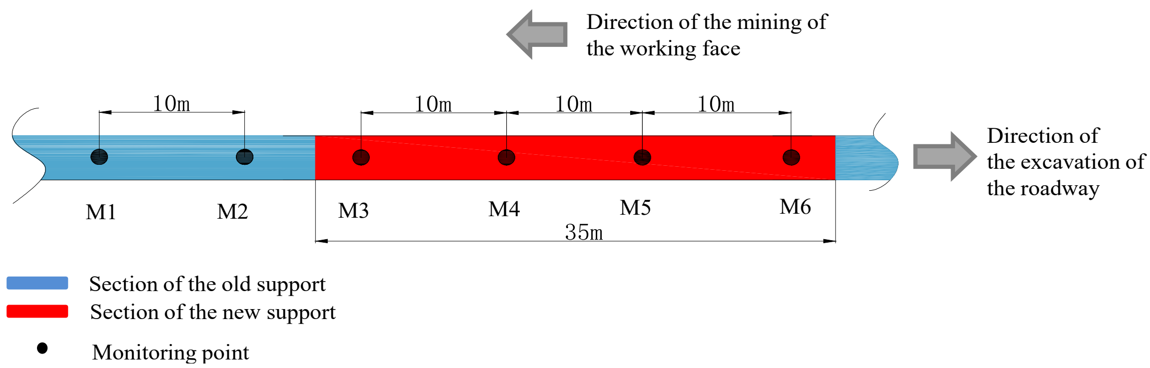

Figure 9. Layout plan of the monitoring points.

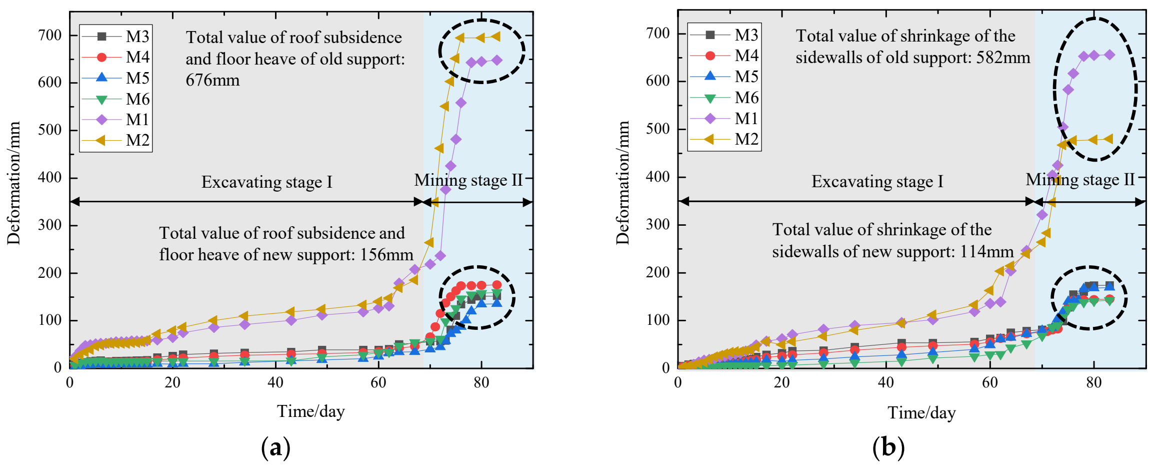

Figure 10. Deformation and time curves of monitoring points: (**a**) roof subsidence and floor heave; (**b**) shrinkage of the sidewalls.

From the monitoring data shown in Figure 10, some results on the deformation value of the roadway can be derived.

(1) New support: In the excavating stage, the average value of the roof subsidence and floor heave was 23 mm, and the average shrinkage of the sidewalls was 30 mm. The time it takes to enter the stable stage of I3 is about 6 days. In the mining stage, the total value of the roof subsidence and floor heave was 156 mm, and the total deformation of the shrinkage of the sidewalls was 114 mm. The time it takes to enter the stable stage of II3 is about 10 days.

(2) Old support: In the excavating stage, the average value of the roof subsidence and floor heave was 101 mm, and the average shrinkage of the sidewalls was 85 mm. The time it takes to enter the stable stage of I3 is about 12 days. In the mining stage, the total value of the roof subsidence and floor heave was 676 mm, and the total deformation of the shrinkage of the sidewalls was 582 mm. The time it takes to enter the stable stage of II3 is about 18 days.

A comparison of the deformation values shows that the total values of the new stability control method were much lower than those under the old stability control method. The total value of the roof subsidence and floor heave in the new support is only about 23.1% of that in the old support. Additionally, the total deformation of the shrinkage of the sidewalls in the new support is only about 19.6% of that in the old support. The average total deformation of the roadway surface in the new support is only about 21.4% of that in the old support. The total time of the support materials entering the stable stages of I3 and II3 in the new support is nearly 53.3% of that in the old support. Therefore, in terms of the surrounding rock deformation in the test section, the proposed coupled stability control method can effectively control the nonlinear large deformation of swelling soft rock roadways in sea areas.

5. Conclusions

(1) On the basis of the X-ray diffraction and electron microscope scanning results, the characteristics of the swelling soft rock can be derived: ① The swelling soft rock had a large proportion of clay minerals, especially smectite and kaolinite; ② massive dissolution holes were found on the surface of the minerals, and part of them were padded with argillaceous components; and ③ the development of microfractures in the rocks is fine, and some of them are well connected, with a portion of them filled with albite, pyrite, and halite.

(2) An on-site investigation derived the following characteristics of large deformation: ① large deformation and overall shrinkage of the roadway; ② persistent deformation; and ③ failure of support materials.

(3) The compound deformation mechanism can be transformed into a simple one through some countermeasures. The design of coupling support that contains an anchor beam, steel mesh, CRLD bolts, floor grouting bolts, and steel fiber concrete was proposed and applied.

(4) By releasing the stresses accumulated by the swelling soft rock, the CRLD bolts control the deformation of the roof and sidewalls effectively. The floor grouting bolt effectively controls the ground uplift by cutting off the slip line of the basement angle.

(5) The average total deformation of the roadway surface in the new support is only about 21.4% of that in the old support. The total time of the support materials entering the stable stages of I3 and II3 in the new support is nearly 53.3% of that in the old support. The proposed coupling stability control method can effectively control the nonlinear large deformation of the swelling soft rock. This approach can be taken as a good reference for the nonlinear large-deformation mechanism and stability control of swelling soft rock roadways in sea areas.

Author Contributions: Conceptualization, X.S. and D.W.; methodology, D.W. and Y.J.; validation, H.L. and F.C.; formal analysis, D.W. and H.X.; writing—original draft preparation, D.W. and L.D.; writing—review and editing, D.W. and B.L. All authors have read and agreed to the published version of the manuscript.

Funding: This research was funded by the National Natural Science Foundation of China (No. 51874311, 52204101), the Natural Science Foundation of Shandong Province (No. ZR2022QE137, ZR2022QE212), and the Open Project of State Key Laboratory for Geomechanics and Deep Underground Engineering in CUMTB (No. SKLGDUEK2023).

Institutional Review Board Statement: Not applicable.

Informed Consent Statement: Not applicable.

Data Availability Statement: All data and models generated or used during the study appear in the submitted article.

Conflicts of Interest: The authors declare no conflict of interest.

References

1. BP p.l.c. *BP Statistical Review of World Energy 2022*; BP p.l.c.: London, UK, 2022.
2. China National Bureau of Statistics. *Statistical Bulletin on National Economic and Social Development 2022*; China National Bureau of Statistics: Beijing, China, 2022.
3. Development Strategy and Planning Division of the National Development and Reform Commission. *The Outline of the 14th Five-Year Plan for National Economic and Social Development and Vision 2035 of the State and All Regions*; People's Press: Beijing, China, 2022.

4. Institute of Resources and Environmental Policy of Development Research Center of The State Council. *Progress Report on China's Energy Revolution*; Petroleum Industry Press: Beijing, China, 2022.
5. Miao, X.; Liu, W.; Chen, Z. *Seepage Theory of Mining Rock Mass*; Science Press: Beijing, China, 2004.
6. Wu, X.; Yu, Q.; Wang, X.; Duan, Q.; Li, X.; Yang, J.; Bao, Y. Exploitation of coal resources under surface water body. *Chin. J. Rock Mech. Eng.* **2006**, *25*, 1029–1036.
7. Feng, F.; Chen, S.; Wang, Y.; Huang, W.; Han, Z. Cracking mechanism and strength criteria evaluation of granite affected by intermediate principal stresses subjected to unloading stress state. *Int. J. Rock Mech. Min. Sci.* **2021**, *143*, 10473. [CrossRef]
8. Chen, S.; Feng, F.; Wang, Y.; Li, D.; Jiang, N. Tunnel failure in hard rock with multiple weak planes due to excavation unloading of in-situ stress. *J. Cent. South Univ.* **2020**, *27*, 2864–2882. [CrossRef]
9. Feng, F.; Xie, Z.; Xue, T.; Wang, E.; Huang, R.; Li, X. Application of a combined FEM/DEM approach for teaching a deep rock mass mechanics course. *Sustainability* **2023**, *15*, 937. [CrossRef]
10. Xie, H.; Gao, F.; Ju, Y. Research and Development of Rock Mechanics in Deep Ground Engineering. *Chin. J. Rock Mech. Eng.* **2015**, *34*, 2161–2178.
11. He, M.; Xie, H.; Peng, S.; Jiang, Y. Study on Rock Mechanics in Deep Mining Engineering. *Chin. J. Rock Mech. Eng.* **2015**, *24*, 2803–2813.
12. Xie, H. Research Framework and Anticipated Results of Deep Rock Mechanics and Mining Theory. *Adv. Eng. Sci.* **2017**, *49*, 1–16.
13. Yuan, L. Strategic Thinking of Simultaneous Exploitation of Coal and Gas in Deep Mining. *J. China Coal Soc.* **2016**, *41*, 1–16.
14. Kang, H. Support Technologies for Deep and Complex Roadways in Underground Coal mines: A Review. *Int. J. Coal Sci. Tech.* **2014**, *1*, 261–277. [CrossRef]
15. He, M. Progress and challenges of soft rock engineering in depth. *J. China Coal Soc.* **2014**, *39*, 1409–1417.
16. He, M.; Gong, W.; Wang, J.; Qi, P.; Tao, Z.; Du, S.; Peng, Y. Development of a novel energy-absorbing bolt with extraordinarily large elongation and constant resistance. *Int. J. Rock Mech. Min. Sci.* **2014**, *67*, 29–42. [CrossRef]
17. Sun, X.; Zhang, Y.; Wang, D.; Yang, J.; Xu, H.; He, M. Mechanical properties and supporting effect of CRLD bolts under static pull test conditions. *Int. J. Rock Mech. Min. Sci.* **2017**, *24*, 1–9. [CrossRef]
18. Sun, X.; Wang, D.; Wang, C.; Liu, X.; Zhang, B.; Liu, Z. Tensile properties and application of constant resistance and large deformation bolts. *Chin. J. Rock Mech. Eng.* **2014**, *33*, 1765–1771.
19. Wang, D.; Jiang, Y.; Sun, X.; Luan, H.; Zhang, H. Nonlinear Large Deformation Mechanism and Stability Control of Deep Soft Rock Roadway: A Case Study in China. *Sustainability* **2019**, *11*, 6243. [CrossRef]
20. Yang, X.; Pang, J.; Liu, D. Deformation mechanism of roadways in deep soft rock at Hegang Xing'an coal Mine. *Int. J. Min. Sci. Tech.* **2013**, *23*, 307–312. [CrossRef]
21. He, M.; Gao, Y.; Yang, J.; Gong, W. An Innovative Approach for Gob-Side Entry Retaining in Thick Coal Seam Longwall Mining. *Energies* **2017**, *10*, 1785. [CrossRef]
22. He, M.; Jing, H.; Sun, X. *Soft Rock Engineering Mechanics*; Science Press: Beijing, China, 2002.
23. He, M.; Sun, X. *Support Design and Construction Guide of Soft Rock Roadway Engineering in Chinese Coal Mines*; Science Press: Beijing, China, 2004.
24. He, M. Conception system and evaluation indexes for deep engineering. *Chin. J. Rock Mech. Eng.* **2005**, *24*, 2853–2858.
25. Zhang, N.; Liu, L.; Hou, D.; He, M.; Liu, Y. Geomechanical and water vapor absorption characteristics of clay-bearing soft rocks at great depth. *Int. J. Min. Sci. Tech.* **2014**, *24*, 811–818. [CrossRef]
26. Guo, Z.; Wang, H.; Ma, Z.; Wang, P.; Kuai, X.; Zhang, X. Research on the Transmission of Stresses by Roof Cutting near Gob Rocks. *Energies* **2021**, *14*, 1237. [CrossRef]
27. Ma, Z.; Wang, Y.; Huang, L.; Wang, H.; Wang, J.; Wang, Z.; Wang, Y.; Wang, B. Research on the Stability Mechanism of the Surrounding Rock of Gob-Side Entry Retaining by Roof Cutting in Dianping Coal Mine. *Minerals* **2022**, *12*, 965. [CrossRef]
28. Guo, H.; Li, B.; Zhang, Y.; Wang, X.; Zhang, F. Hydrophilic characteristics of soft rock in deep mines. *Int. J. Min. Sci. Technol.* **2015**, *25*, 177–183. [CrossRef]
29. Yang, X.; Wang, J.; Zhu, C.; He, M.; Gao, Y. Effect of wetting and drying cycles on microstructure of rock based on SEM. *Environ. Earth Sci.* **2019**, *78*, 1–10. [CrossRef]
30. Guo, H.; Zhao, J.; Liu, P. Experimental studies and chemical analysis of water on weakening behaviors of deep soft rock. *Chin. J. Rock Mech. Eng.* **2018**, *37*, 3374–3381.
31. He, M.; Yang, X.; Sun, X. *Study on Clay Mineral Characteristics for Soft Rock of Coal Mine in China*; China Coal Industry Publishing House: Beijing, China, 2006.
32. Sun, X.; He, M.; Yang, X. Research on nonlinear mechanics design method of bolt-net-anchor coupling support for deep soft rock tunnel. *Rock Soil Mech.* **2006**, *27*, 1061–1065.